Microfluid Nanofluid
DOI 10.1007/s10404-011-0887-1

RESEARCH PAPER

Surface infusion micropatterning of elastomeric substrates

Huipeng Chen · Daniel M. Lentz · Alicyn M. Rhoades · Robert A. Pyles · Karl W. Haider · Siva A. Vanapalli · Ryan K. Nunley · Ronald C. Hedden

Received: 26 July 2011 / Accepted: 21 September 2011

Abstract Surface infusion micropatterning (SIM) is a novel microfabrication process for simultaneous topographical and chemical patterning of elastomeric substrates. The SIM process involves three steps: (1) infusion of a monomer into the substrate, (2) photopolymerization through a patterned contact mask, and (3) drying. For the first time, SIM is demonstrated to create wells and channels (typical depth 5–22 μm, width 20–200 μm) in two substrate materials, a crosslinked polydimethylsiloxane elastomer and a thermoplastic polyurethane elastomer. High-resolution surface features produced include a "checkerboard" well pattern and a microfluidic channel system. The surface micropatterns have been characterized by scanning electron microscopy, optical microscopy, and optical profilometry to quantify channel depth and shape. Because of wall curvature effects, SIM is most suitable for producing shallow (aspect ratio <0.5) microfluidic channels in soft elastomeric materials. Due to the different chemical composition of the interpenetrating polymer network formed in the exposed regions, SIM also produces surface chemical patterning, as illustrated by selective dye-staining experiments. The potential for SIM to impact emerging technologies is discussed in the light of process advantages and limitations.

Keywords Elastomers · Infusion · Microfabrication · Microfluidics

1 Introduction and background

The last decade has witnessed revolutionary advances in the fields of microfabrication and microfluidics (Stone 2004; Squires 2005; Whitesides 2006) because of a number of attractive attributes of miniaturization, such as conservation of material in biological analyses. Microfluidic devices have found applications in a variety of fields including cell and molecular biology, (Vanapalli 2009; Andersson 2003; El-Ali 2006) medicine, (Toner 2005; Yager 2006) synthesis of novel materials, (Shah 2008; Dendukuri 2009) biosensors (Kim 2009; Liu 2010) and food safety. (Skurtys 2008). In recent years, microfabrication procedures have shifted from substrate materials such as silicon or glass toward inexpensive polymers that may be preferable for mass production of disposable devices. (Becker 2002). The development of accessible processing methods for microscale patterning of soft elastomeric materials such as poly(dimethylsiloxane) (PDMS) (McDonald 2000) has led to an explosive growth in research into microfluidic devices and microcontact printing devices. "Soft lithography" has revolutionized research in academic laboratories, where fabrication of PDMS devices by simple casting protocols proves cost effective (Becker and Gartner 2008). However, scale-up of new devices from the prototype stage to the mass production stage can require a change in both materials and equipment, a hindrance to commercialization (Becker and Gartner 2008).

H. Chen · S. A. Vanapalli · R. K. Nunley · R. C. Hedden (✉)
Department of Chemical Engineering, Texas Tech University, Lubbock, TX 79409, USA
e-mail: ronald.hedden@ttu.edu

D. M. Lentz
Department of Materials Science and Engineering, The Pennsylvania State University, University Park, PA 16802, USA

A. M. Rhoades · R. A. Pyles · K. W. Haider
Bayer Material Science LLC, Pittsburgh, PA 15205, USA

Published online: 13 October 2011

Other microfabrication processes for polymers include photolithography, (Burns 1998; Harrison 2004; Haraldsson 2006; Lin 2002; Sikanen 2005; Tuomikoski 2005; Gadre 2004; Nijdam 2005; Liu et al. 2003; Ribeiro et al. 2005; Tay et al. 2001; Lin et al. 2002; Yu et al. 2006; Metz et al. 2004; Sato et al. 2006; Agirregabiria et al. 2005; Abgrall et al. 2006; Yu et al. 2006; Alderman et al. 2001) casting, (McDonald et al. 2000; Whitesides et al. 2001; Sia and Whitesides 2003; Gates et al. 2005; Kumar and Whitesides 1993; Xia and Whitesides 1998; Kim et al. 1996; Kim et al. 1997) injection molding, (Giselbrecht et al. 2006; McCormick et al. 1997; Giboz et al. 2007; Yu et al. 2002; Hulme et al. 2002; Svedberg et al. 2003; Han et al. 2003; Noerholm et al. 2004; Ahn et al. 2004; Xu et al. 2005; Kim et al. 2006; Mair et al. 2006; Nikcevic et al. 2007) microthermoforming, (Giselbrecht et al. 2006), hot embossing (Armani and Liu 2000; Barker et al. 2000; Becker and Heim 2000; Galloway et al. 2002; Heckele et al. 1998; Juang et al. 2002a, b; Kameoka et al. 2001, 2002; Kricka et al. 2002; Liu et al. 2001; Meng et al. 2001; Qu et al. 2006; Rowland and King 2004; Scheer and Schulz 2001; Schulz et al. 2003; Young 2005), and contact liquid photolithographic polymerization (CLiPP). (Haraldsson et al. 2006; Hutchison et al. 2004) Several of these processes may be more adaptable to high-throughput manufacturing, but some are less attractive to labs engaged in rapid prototyping of new devices because of the costs associated with mold fabrication or processing equipment.

A single process that allows rapid, cost-efficient production of micropatterned polymer devices at both the lab scale and the industrial scale could prove invaluable to microfabrication science and industry. Surface infusion micropatterning (SIM) is a new microfabrication process for surface relief patterning of transparent elastomeric substrates, including both chemically crosslinked or vulcanized materials (e.g., polydimethylsiloxane, PDMS) and thermoplastic elastomers (e.g., thermoplastic polyurethanes, TPUs). SIM can be used to produce patterned surface features having dimensions of typical depth of 5–22 μm or more and typical width of 20–200 μm. Patterning of the substrate by SIM is a three-step process (Fig. 1). The substrate should be an optically transparent elastomer, which can be formed into a thin sheet with very flat surface. The substrate may be either free-standing or mounted on glass or another rigid material. The elastomer is soaked in a polymerizable, liquid monomer in the first step. The infused monomer is subsequently photopolymerized by ultraviolet (UV) irradiation through a contact mask to create a patterned interpenetrating or semi-interpenetrating network (IPN or sIPN) within the surface. Finally, the residual monomer is removed by evaporation, creating channels or wells in the surface due to shrinkage.

A key feature of the SIM process is its applicability to diverse substrate materials, which provides substantial freedom to tune mechanical properties, optical properties, chemical resistance, and resistance to biological fouling to match the intended application. A second key advantage of SIM is that minimal equipment and materials are needed; there is no requirement for elaborate instrumentation or tooling of expensive molds. SIM is therefore readily amenable to rapid prototyping of new devices. A third advantage of SIM is its ability to produce simultaneous topographical and chemical patterning of the surface due to the different chemical composition of the IPN regions. The presence of surface-accessible functional groups in the raised IPN regions will be demonstrated in this work.

The SIM process differs fundamentally from a photopatterning method reported by Wang et al. (2005) who grafted poly(acrylic acid) onto PDMS elastomer by photopolymerization to achieve patterned relief features, taking advantage of an intervening IPN layer to achieve adhesion. In SIM, no liquid monomer is present on the surface during photopolymerization, and the surface relief pattern is formed by shrinkage of the swollen substrate in unexposed regions, not by grafting of residual photopolymerized material to the surface. We are not presently aware of other techniques that resemble SIM.

This report concerns the first demonstration of SIM with two representative elastomeric substrates, a chemically crosslinked PDMS and a thermoplastic polyurethane (TPU). SIM is employed to create high-resolution surface features, including a "checkerboard" well pattern and a microfluidic channel system. Key processing variables affecting the depth and cross-sectional shape of the resulting features are identified. A systematic study of monomer uptake versus time allows estimation of monomer diffusivity, from which the concentration profile of infused monomer inside the elastomeric substrate is calculated via Fick's Law. Gravimetric measurements characterize the fraction of infused monomer that is converted to polymer. The surface micropatterns are examined by SEM, optical microscopy, and optical profilometry to characterize channel depth and shape. SIM is shown to be suitable for producing shallow (height/width <0.5) microfluidic channels in elastomers of widely varying chemical composition, including both chemically crosslinked and thermoplastic types. The presence of patterned surface functional groups is demonstrated by staining of a patterned poly(methacrylic acid) sIPN in a PDMS elastomer with a fluorescent dye. Considering process advantages and limitations, the potential for SIM to impact emerging technologies is discussed.

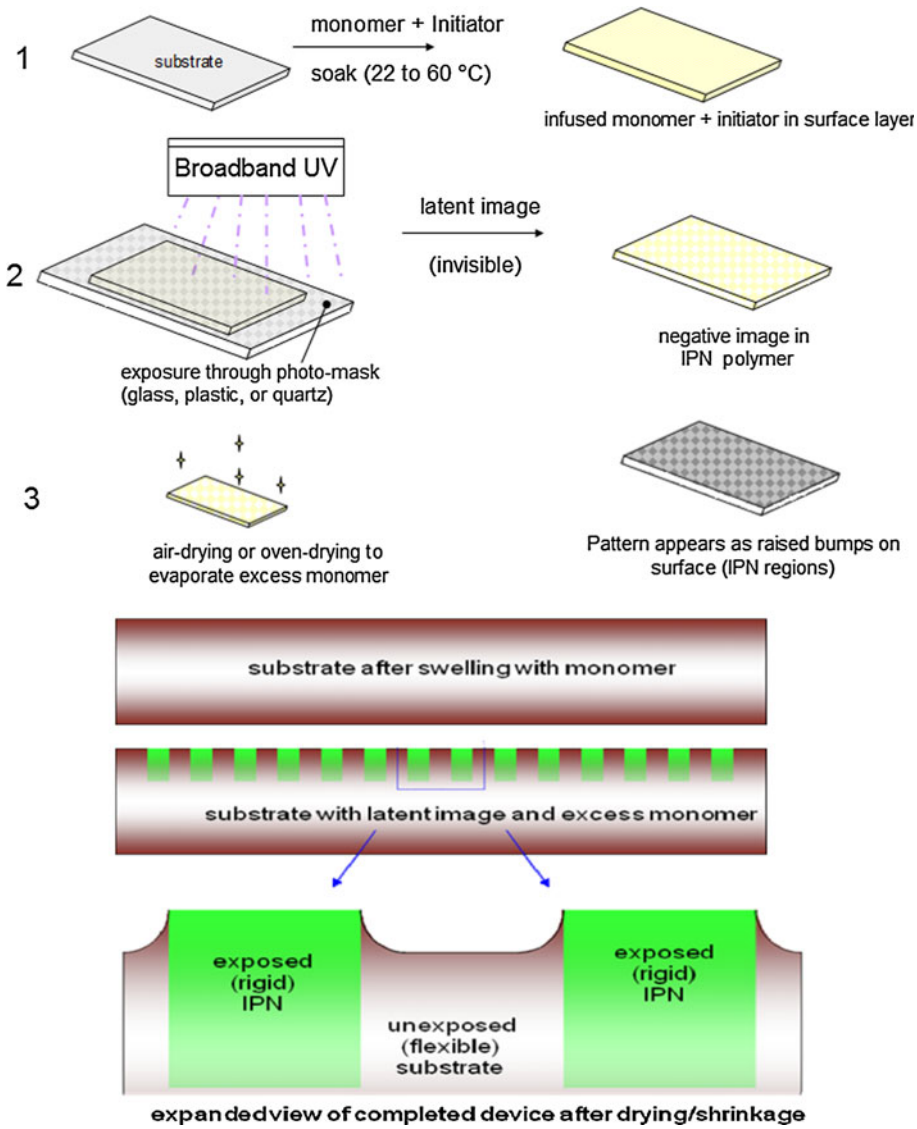

Fig. 1 Schematic of steps in SIM process

2 Experiments

2.1 Chemicals and materials

Methacrylic acid (MAA, 99.5%, stab. with 250 ppm 4-methoxyphenol, ACROS), ethylene glycol dimethacrylate (EGDMA, 98%, stab. with 100 ppm 4-methoxyphenol, Alfa Aesar), methyl methacrylate (MMA, 99%, Alfa Aesar), hydroxyethylmethacrylate (HEMA, 97%, stab. with ca. 500 ppm 4-methoxyphenol), and pentaerythritol triacrylate (PETA, stab. with ca. 300–400 ppm 4-methoxyphenol, Alfa Aesar) were used as received, without removing inhibitors. 2,2-dimethoxy-1,2-diphenylethan-1-one (Irgacure® 651, Ciba) was used as received. TPU Texin® DP7-1196 was obtained as a gift from Bayer MaterialScience (Pittsburgh PA) as an extruded sheet with a thickness of 0.32 mm. The pre-polymer and the crosslinker for a commercial PDMS elastomer were Sylgard 184 (Dow Corning, purchased as a kit). The two components were mixed in a 10:1 ratio (w:w) and degassed in vacuum at room temperature for 20 min to eliminate air bubbles. The viscous mixture was poured onto a polished silicon wafer and cured at 60°C for 12 h in air to obtain a slab of PDMS elastomer having an ultra-flat surface on one side and an approximate thickness of 3.2 mm.

2.2 Monomer sorption kinetics

Infusion of methacrylate monomers into the TPU and PDMS materials was characterized by a standard gravimetric sorption technique. A flat sheet of the elastomer of 3.0 × 3.0 cm top surface area and 0.32 mm thickness (TPU) or 3.2 mm thickness (PDMS) was immersed in pure monomer at a controlled temperature and removed after a

known immersion time t_i. After drying of the surface with a lint-free wiper, the sample's mass was recorded immediately. The evaporation of the monomer from the elastomer was sufficiently slow to allow accurate and repeatable measurements of the monomer mass uptake versus t_i using an ordinary laboratory balance. To avoid cumulative errors resulting from removal/re-immersion of the same sample, a different piece of elastomer was used for each t_i, up to a maximum immersion time of 30–60 min. The mass uptake of the elastomer reached a constant value typically after 1–5 days of immersion, and the mass at equilibrium swelling (M_∞) was taken as the final recorded mass.

2.3 Instrumentation

Scanning electron microscope (SEM) imaging was performed on gold–coated samples with a HITACHI S-3400N SEM operated at 5 kV. Optical microscope images were taken with an Olympus BX51 light microscope equipped with 5×, 20×, and 50× strain-free objectives. Fluorescence microscopy was conducted with an Olympus IX71 fluorescence microscope equipped with Simple PCI software. UV–Vis spectra were recorded with a Shimadzu UV-2550 spectrophotometer at room temperature. The channel depth and shape of micropatterned features were characterized with a Dektak 3030 surface profiling measuring system from Sloan Technology Corporation. The micropatterned features were also imaged by a Veeco Wyko NT1100 Optical Profiling System after sputtering a thin layer of Au onto the samples' surfaces to increase reflectivity.

2.4 Mounting of thermoplastic polyurethane elastomer on glass

The TPU material was typically mounted on a glass microscope slide before SIM processing. A 1.5 × 1.5 cm square piece of TPU (0.32 mm thickness) was cut from the sheet provided by the supplier. The TPU was placed on top of an untreated glass slide, which was heated to 178°C for 2 min on a hot stage. During the melting procedure, a second glass slide with a hydrophobic surface was placed on top of the TPU. The hydrophobic slide was prepared beforehand by treating with a silane coupling agent, *n*-octadecyltrimethoxysilane (95%, Gelest, Inc.) in an acidified water–ethanol mixture, followed by curing in air for 10 min at 110°C, according to the manufacturer's instructions. Compression of the molten TPU was minimized by insertion of two glass spacers of equal thickness between the glass slides. The TPU and glass slides were cooled to room temperature, and the hydrophobic glass slide was easily removed from the TPU, leaving a very flat surface that was suitable for micropatterning. The TPU material adhered strongly to the lower (untreated) slide, such that it did not peel off during any stage of SIM processing.

2.5 SIM processing

An example of a typical SIM processing procedure is described. (Monomer soak times and UV exposure times for individual samples are specified in the text.) A slab of the elastomeric substrate was immersed in a solution of (99% w/w monomer, 1.0% w/w Irgacure® 651) at room temperature for several min, after which the sample surfaces were dried by patting with a lint-free wiper until no liquid monomer was visible. A photomask was placed in contact with the top surface of the substrate material. As intimate contact between the mask and sample surface was vital to achieving pattern transfer, a compressive force of up to 5.5 N/cm^2 was applied to the sample's surface during exposure by placing weights on top of the mask. The swollen substrate material and mask were transferred to a plastic exposure box with a transparent quartz top window. The sample was irradiated with a BLAK–RAY long-wavelength UV lamp, Model B 100AP, (Cole-Parmer) with 100 W Sylvania H44GS-100M Mercury Lamp bulb at an approximate distance of 12.5 cm from the sample's surface for typically 10 min, during which time the exposure box was continuously flushed with N_2. The maximum UV dose rate at the center or the illuminated area was measured to be 0.041 ± 0.02 W/cm^2, providing an approximate dose of 25 J/cm^2 for a typical 10 min exposure. After exposure, the sample's mass was recorded, and it was dried in air at room temperature until its mass was no longer decreasing measurably. After drying, to make the micropatterned surface more hydrophilic, the material could optionally be exposed to UV-ozone treatment in a Harrick PDC-326 plasma cleaner for 2–5 min. A series of non-patterned samples was also prepared by omitting the photomask in the processing sequence. These samples were used to quantify conversion of monomer to polymer.

2.6 Staining and imaging of patterned sample

A PDMS elastomer was infused with methacrylic acid and photoinitiator for 10 min at ambient temperature, followed by exposure to UV radiation for 5 min through a quartz mask with a 40 μm checkerboard pattern. Poly(MAA) sIPN regions were selectively stained with a fluorescent dye, 6-aminofluorescein, to demonstrate chemical micropatterning of the surface. The patterned elastomer was immersed in an aqueous solution of 0.1% w/w 6-aminofluorescein (Sigma-Aldrich) for 10 min, dried, and imaged in a fluorescence microscope equipped with a fluorescein filter. The incident wavelength was 495 nm and the

observation wavelength was 528 nm. The amine groups of the dye bind to the –COOH groups of poly(methacrylic acid), but the dye does not bind to PDMS. (Wang et al. 2005).

3 Results and discussion

3.1 Infusion fundamentals

The first step in SIM processing (illustrated schematically in Fig. 1) is the infusion of a polymerizable monomer into the substrate. The elastomer is immersed in a liquid monomer bath, exposing one side (if glass-mounted) or both sides (if free-standing) to the liquid. Approximately 1.0% w/w of a free-radical photoinitiator compound is dissolved in the (liquid) monomer, but no solvents are present. Both the monomer and the dissolved photoinitiator begin to diffuse into the elastomer, which is held at a temperature above its glass transition. Enough of the photoinitiator diffuses into the elastomer with the monomer to allow photopolymerization in the subsequent step. After the infusion of monomer and photoinitiator is complete, the surfaces are wiped clean by suitable mechanical means to remove excess liquid.

Preferred monomers include, but are not limited to, the various acrylates and methacrylates listed in Table 1. Choice of monomer depends on the desired rate and depth of infusion, the preference for volatility or non-volatility, the desired final mechanical properties of the device, and the desire for hydrophobic or hydrophilic surface character. The monomer must be a thermodynamically "good" solvent for the substrate, so there is a significant driving force for the monomer to swell the elastomer. If the substrate is a thermoplastic elastomer, it must not dissolve in the monomer or melt at the processing temperature, however.

The amount of infused monomer strongly affects the final feature characteristics, so characterization of the monomer infusion process at a fundamental level is essential to understanding and optimizing the process. Infusion kinetics for several monomers were therefore characterized in both TPU and PDMS by gravimetric sorption experiments. The elastomer samples were assumed to swell in each monomer at constant temperature, such that Fickian diffusion into both top and bottom surfaces occurred simultaneously. Diffusion into the sides was neglected. M_t is the mass of the slab at time t_i, M_0 is its initial (dry) mass, and M_∞ is its equilibrium swollen mass. For $(M_t - M_0)/(M_\infty - M_0) \ll 0.5$, the sorption data are expected to follow Eq. 1 (Crank 1968):

$$\frac{M_t - M_0}{M_\infty - M_0} \approx 2\left(\frac{D_{12}}{\pi L^2}\right)^{1/2} t_1^{1/2} \quad (1)$$

In Eq. 1, D_{12} is the diffusivity of the monomer in the elastomer and $2L$ is the full thickness of the slab. Edge effects are assumed to be negligible. Figure 2a illustrates gravimetric sorption data for the diffusion of different monomers into the TPU. A linear least-squares fit to the data in Fig. 2a yields D_{12} values from the slope (Table 2). The MMA has the highest diffusivity, while PETA has the lowest. Figure 2b illustrates gravimetric sorption data for a single monomer (MAA) into PDMS elastomer with $D_{12} = 1.29 \times 10^{-6}$ cm^2/s. The other monomers listed in Table 1 were not studied with PDMS because of very low infusion rate (PETA and HEMA), or because of the incompatibility of PDMS with the resulting polymers, leading to microphase separation and an opaque appearance (MMA and EGDMA). The TPU material allowed a more diverse selection of monomers to be infused than PDMS.

The concentration profile of the infused monomer can be estimated from Fick's Law using the measured diffusivities. Assuming the chemical composition of the host polymer and its morphology are depth-independent, and assuming that the elastomer is well above its T_g at the infusion temperature, the concentration profile of the

Table 1 List of preferred monomers and their properties

Monomer (abbreviation)	Monomer boiling pt.	Attributes
Methyl methacrylate (MMA)	101°C	Linear polymer $T_g \approx$ 95–105°C. Rapid infusion; volatile
Methacrylic acid (MAA)	161°C	Linear polymer, $T_g \approx$ 156°C. Hydrophilic, hydrogen bonding
Ethylene glycol dimethacrylate (EGDMA)	99°C	Homopolymer is crosslinked thermoset (rigid).
Hydroxyethylmethacrylate (HEMA)	67°C	Linear polymer $T_g \approx$ 55–87°C Somewhat hydrophilic.
Pentaerythritol triacrylate (PETA)	210°C (approximate)	Homopolymer is crosslinked thermoset (rigid). Low monomer volatility; slow infusion.

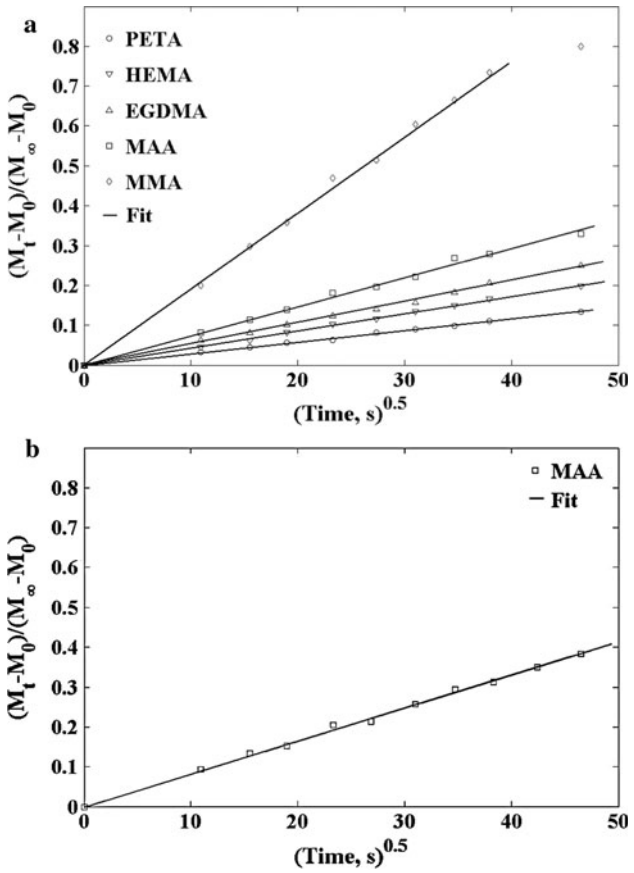

Fig. 2 **a** Sorption of different monomers into the TPU during soaking at 22°C. **b** Sorption of MAA monomer into the PDMS elastomer during soaking at 22°C. Each line is a best fit to the data with forced intercept = 0

monomer versus depth within the PDMS plate at soak time t_1 can be estimated by Eq. 2 (Crank 1968).

$$C = (C_s)\mathrm{erfc}\left(\frac{y}{2\sqrt{(D_{12}t_1)}}\right) \quad (2)$$

In Eq. 2, C_s is the surface concentration of monomer, which is assumed to equal its concentration at the equilibrium swelling condition, and y is the depth below the surface. C_s was determined for each elastomer/monomer pair by allowing the elastomer to swell to equilibrium in the monomer and recording its mass (Table 2). Deviations from Eq. 2 might be observed due to orientation effects arising from processing history, in which case D_{12} would depend on depth. However, we shall consider here the simplest case of a homogeneous substrate in order to estimate the depth of infusion of the monomer. Figure 3a, b present the monomer concentration profiles beneath the surface for infusion of MAA into TPU and PDMS elastomers, respectively. Samples were assumed to be thick enough such that infusion profiles from the two sides did not overlap. From Fig. 3a, b, the approximate infusion depth of the MAA monomer after a 15 min soak was about 100 μm for the TPU material and 1 mm for the PDMS, taking the "depth of penetration" arbitrarily to be the value of y at which $C = 1\%$ w/w. In both cases, for 15 min soak times, the depth of penetration of the monomer was less than half of the film's thickness. Measured values of D_{12} and C_s for the various monomers in the TPU are listed in Table 2.

A short monomer soak time is desirable, so the monomer should ideally possess both a high D_{12} in the substrate and a high solubility (C_s). C_s and D_{12} are also key parameters governing the maximum achievable depth of channels or wells in the surface. The shrinkage of the substrate due to evaporation of the monomer produces the surface relief features, so a substantial volume fraction of monomer must be infused quickly in order to produce well-defined channels or wells. Volatility is another key consideration affecting ease of processing. Volatile monomers may be more difficult to process during the UV exposure step due to rapid evaporation from the surface. On the other hand, high volatility may be helpful by accelerating the final drying step. The monomers listed in Table 2 vary considerably in solubility, diffusivity, and volatility, but all provided satisfactory performance under some set of conditions.

3.2 Photopolymerization

The second step involves pseudo-lithographic exposure of the monomer-infused elastomer sheet with broadband ultraviolet (UV) light through a negative-tone contact mask to create a latent image. After infusion of the monomer, the swollen elastomer is immediately transferred to an inert gas chamber and subjected to photopolymerization. The UV light source need not be collimated or monochromatic. During the UV exposure step, a pattern is transferred to the

Table 2 The (equilibrium) surface concentration of monomer (C_s), diffusivity of the monomer (D_{12}), and the mass fraction of monomer converted to polymer, ϕ_c, for several monomers in the TPU elastomer at 22°C

	MMA	MAA	EGDMA	HEMA	PETA
C_s (no units)	0.489 ± 0.002	0.556 ± 0.002	0.374 ± 0.002	0.576 ± 0.002	0.136 ± 0.002
D_{12} ($\times 10^{-8}$ cm^2/s)	7.38 ± 0.03	1.08 ± 0.02	0.57 ± 0.02	0.36 ± 0.01	0.17 ± 0.01
ϕ_C (no units)(%)	93 ± 2	92 ± 2	99 ± 2	91 ± 2	98 ± 2

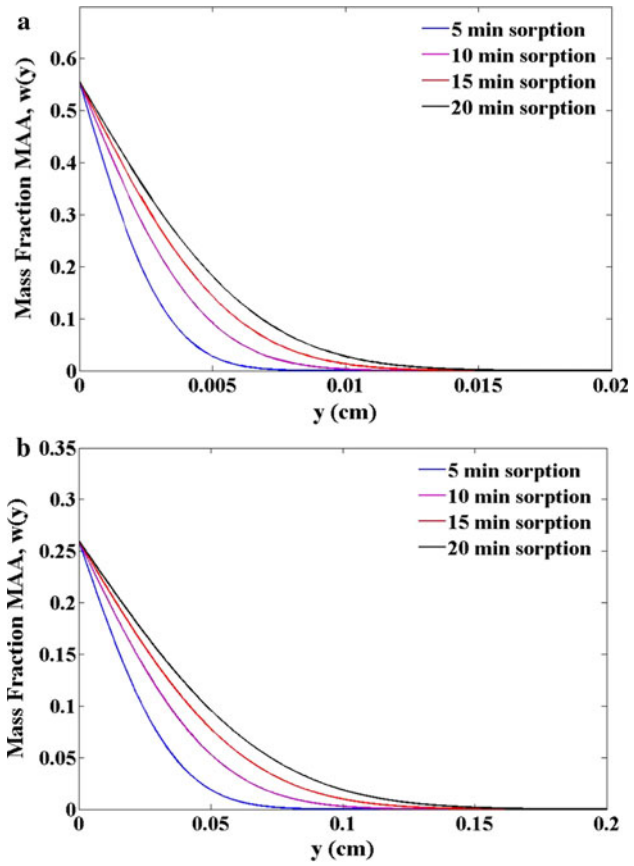

Fig. 3 Calculated concentration profiles of MAA monomer in **a** the TPU elastomer, and **b** the PDMS elastomer, after soak times of 5, 10, 15, and 20 min at 22°C. Initial sample thickness was taken as 0.32 mm for TPU and 3.2 mm for PDMS

substrate by the use of a contact mask, which should be made of a material that is resistant to chemical attack by the infused monomer. Low-cost, disposable plastic masks (generally made of a transparent polyolefin) are usually suitable, but it is also possible to use a quartz/chrome mask, which offers better chemical resistance, if needed. Intimate contact between the mask and the swollen elastomer is necessary for effective pattern transfer. The contact mask also discourages evaporation of monomer during exposure. The UV exposure step ranges in length from a few seconds to several minutes, depending on the rates of initiation and polymerization of the system in question, the UV absorbance of the substrate material, and the rate of decomposition of the radical initiator. Only one side of the substrate is exposed. During UV exposure, the monomer is converted to either a linear polymer, creating a sIPN in the exposed areas, or a crosslinked thermoset, creating an IPN in the exposed areas. The monomer and initiator in the unexposed regions are not converted to polymer. After drying, the exposed regions form raised features, while the unexposed regions form channels or wells.

For all monomers tested with the TPU substrate, photopolymerization was successful, as evidenced by the retention of some part of the infused monomer mass after drying. A high conversion of monomer to polymer is desirable to obtain features of maximum depth and to minimize the amount of monomer that must be removed during the drying step. Factors influencing the monomer conversion include the rate of decomposition of the initiator, the rate of polymerization of the monomer at the chosen temperature, and the UV absorbance spectrum of the elastomeric substrate. The optimal UV exposure time therefore differs somewhat for each monomer/elastomer system.

It is therefore of interest to examine the monomer conversion quantitatively under different conditions. Several samples were prepared without photopatterning to examine mass changes in the exposed regions after infusion and after drying. Elastomers were infused with monomer and initiator on one side only, then fully exposed to the UV light source for a fixed time of 10 min with a non-patterned quartz plate in place of the contact mask. The mass of the exposed IPN material was recorded for 3 days thereafter. The fraction of infused monomer that was converted to IPN or sIPN was determined by comparing the dry mass of the sample before infusion to the final mass after infusion, photopolymerization, and 3 days of drying.

Table 2 shows the mass fraction of monomer converted to polymer, ϕ_C, for different monomers in the TPU material. The measured value of ϕ_C is more than 0.90 for all of the monomers. Control samples, which were only soaked in monomer and initiator (without UV exposure), yielded measured values of ϕ_C less than 0.05 after air-drying for 3 days. Although it is not practical to extract the infused polymers or characterize their molar mass, it is reasonable to conclude that an IPN or sIPN was formed during UV irradiation within the surface of the TPU for all monomers studied. A similar procedure was followed to confirm MAA polymerization in the PDMS elastomer. The measured value of ϕ_C was 0.83 ± 0.02.

Besides the amount of monomer infused and the infusion depth, the UV absorbance of the elastomer is a factor that potentially affects the conversion of monomer to IPN or sIPN. During UV exposure, the monomer in the top surface is subject to intense radiation, but the monomer at greater depths may be irradiated to a much lower extent due to the UV absorbance of the intervening material. The depth of penetration of the UV light is therefore a second factor that potentially limits channel or well depth. Figure 4 illustrates UV absorbance profiles of TPU (0.32 mm thickness) and PDMS (3.2 mm thickness) substrates. The PDMS material was relatively transparent to UV light, despite its greater thickness. For the TPU material,

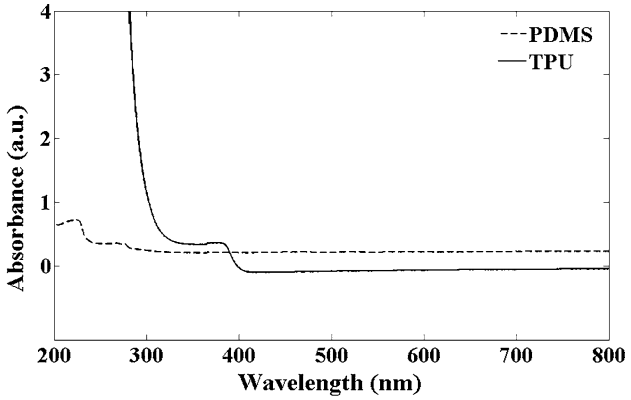

Fig. 4 UV–Vis absorption spectra of TPU (0.32 mm thickness) and PDMS (3.2 mm thickness)

short-wavelength UV light is greatly attenuated as it passes through the slab. Satisfactory micropatterning results were obtained for both elastomeric substrates, suggesting that the UV-transparency of the substrates was not a limiting factor in this study, however.

3.3 Drying

The third and final step in the SIM process is drying by evaporation of the volatile monomer from the unexposed regions. During the drying process, the IPN or sIPN regions shrink minimally, while the unexposed regions swollen with monomer shrink significantly. As a result, high-resolution surface channels or wells are created (illustrated schematically in Fig. 1). The raised features have a different chemical composition than the intervening "trenches" due to the presence of the IPN or sIPN. The raised features may have increased mechanical rigidity compared to the unmodified elastomer, especially if the IPN or sIPN polymer is glassy or densely cross-linked (Lentz 2010). Under the conditions employed in this study, the patterned elastomers were neither brittle nor prone to cracking upon flexion, due to the flexibility of the substrate and the presence of the soft, extensible regions between features.

3.4 Surface feature characterization

Several micropatterned substrates were characterized by SEM, optical microscopy, surface profilometry, and optical profilometry to characterize well or channel depth and shape. Figure 5 shows SEM and optical microscope images of "checkerboard" well patterns in TPU and PDMS substrates. Square wells of width 10, 20, 30, and 40 μm were successfully fabricated in the TPU material using EGDMA, PETA, and MAA monomers. The TPU samples remained transparent to the unaided eye after UV exposure. For the PDMS substrate, the best results were obtained with MAA monomer, which produced a sIPN that was transparent or nearly so. Infusion of PDMS elastomer with EGDMA or PETA resulted in strong microphase separation after UV exposure, judging by the opaque appearance of the samples. As transparency of the device is important in many microfluidic applications, substrate/monomer combinations producing microphase separation are less attractive.

The checkerboard pattern was imaged by optical profilometry after sputtering a layer of Au onto the surface of each sample to increase reflectivity. As shown in Fig. 6, the raised features exhibit high resolution with consistent shape and minimal defects. Surface profilometry was preferred for measurement of well depth because no pretreatment of the surface with Au was necessary. Measured well depth was approximately 2.5 μm in a checkerboard-patterned PDMS elastomer with MAA sIPN features (3 min monomer soak time), and the depth increased to 5.1 μm for a similar sample having MAA soak time of 5 min. Table 3 summarizes the channel depths of PDMS and TPU micropatterned elastomers with varying MAA soak times. The well depths increased steadily with an increase of monomer soak time, indicating that the volume fraction of infused MAA sIPN increased. For a TPU substrate with MAA sIPN features, the channel depth reached 21.7 μm for 30 min soak time, the largest depth achieved in this study.

Figure 7 shows cross-sectional images of a micropatterned PDMS substrate with MAA sIPN features (5 min monomer soak time), which was sectioned with a razor blade perpendicular to the channel direction. The thickness of the visible sIPN layer was approximately 55 μm, and the depth of the channel was about 5 μm. The total width of the channel was about 200 μm. The side-walls of the channel are curved, as the shrinkage of the channel bottom during drying requires stretching of the elastomeric material near the side-walls, producing frozen-in stresses. The curvature of the side-walls affects a portion of the channel bottom of width $\leq$5 μm on each side, while the center of the channel is otherwise quite flat.

Figure 8 shows a channel depth profile for a section of a micropatterned TPU substrate with MAA sIPN features (20 min soak time) and PDMS substrate with MAA sIPN features (30 min soak time). The channel depth ($\sim$16 μm) was uniform, except that significant curvature was again observed in the side walls. SIM is most readily applicable to fabrication of relatively wide (low aspect-ratio) microfluidic channels. Deeper (high aspect-ratio) channels are more likely to exhibit curvature of the walls and channel bottom.

Figure 9a, b shows a finished microfluidic channel system as viewed in an optical microscope (top view). Two

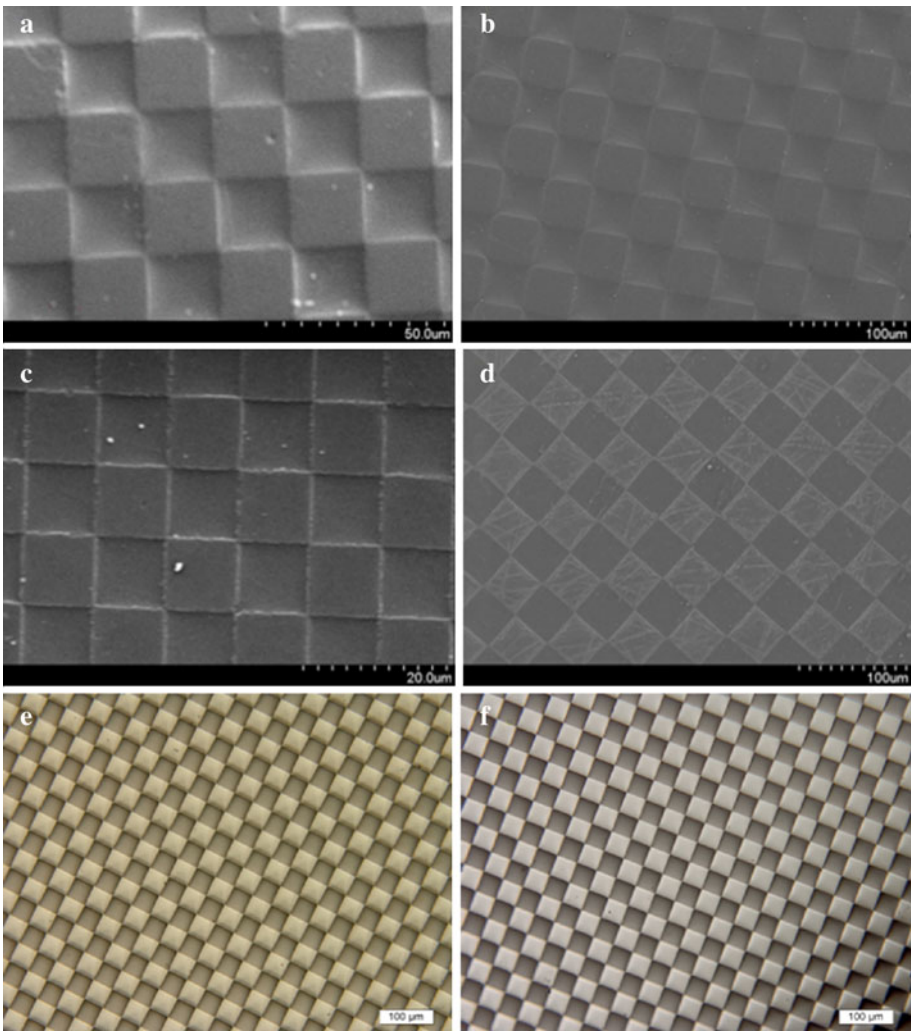

Fig. 5 SEM images and optical microscope images of checkerboard-patterned TPU and PDMS substrates with different IPN patterns. **a** TPU, EGDMA soak 5 min, 20 µm pattern, SEM. **b** TPU, MAA soak 5 min, 40 µm pattern, SEM. **c** TPU, PETA soak 20 min, 10 µm pattern, SEM. **d** PDMS, MAA soak 10 min, 40 µm pattern, SEM. **e** PDMS, MAA soak 10 min, 40 µm pattern, optical microscope. **f** PDMS, MAA soak 20 min, 40 µm pattern, optical microscope

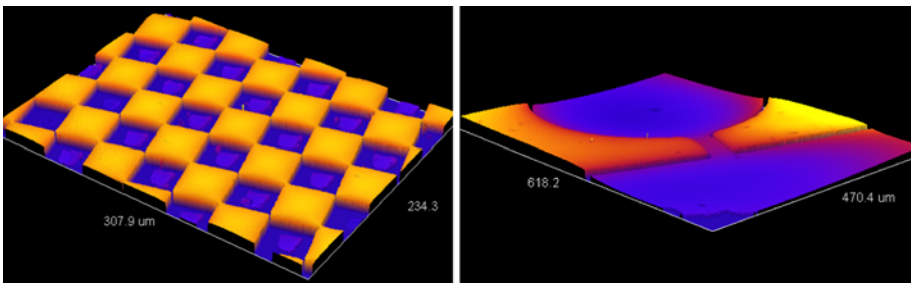

Fig. 6 *Left* optical profilometry depth map for checkerboard-patterned PDMS elastomer, with MAA sIPN features (3 min soak time). *Right* section of a micropatterned PDMS substrate with MAA sIPN features (5 min soak time). Well depths were approximately 7 µm (TPU) and 3 µm (PDMS)

Table 3 Measured channel depths for PDMS and TPU micropatterned substrates with different monomer (MAA) soak times

MAA soak time (min)	Channel depth in PDMS (µm)	Channel depth in TPU (µm)
5	5.1 ± 0.2	10.6 ± 0.2
10	5.7 ± 0.2	14.8 ± 0.2
20	7.0 ± 0.2	16.2 ± 0.2
30	11.0 ± 0.2	21.7 ± 0.2

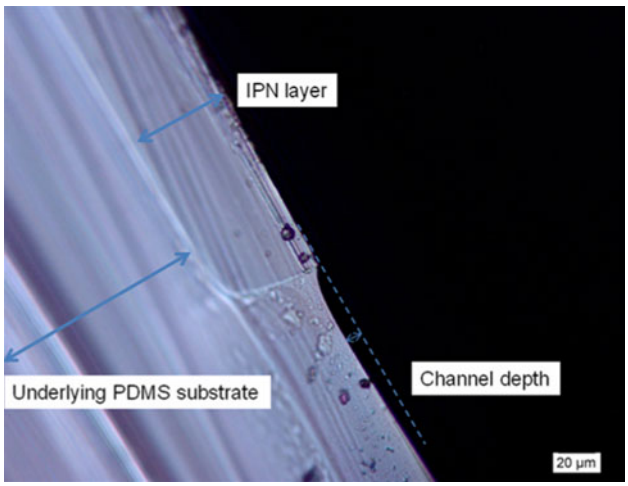

Fig. 7 Microscope images of the cross-section of a micropatterned PDMS substrate with MAA sIPN features (5 min soak time)

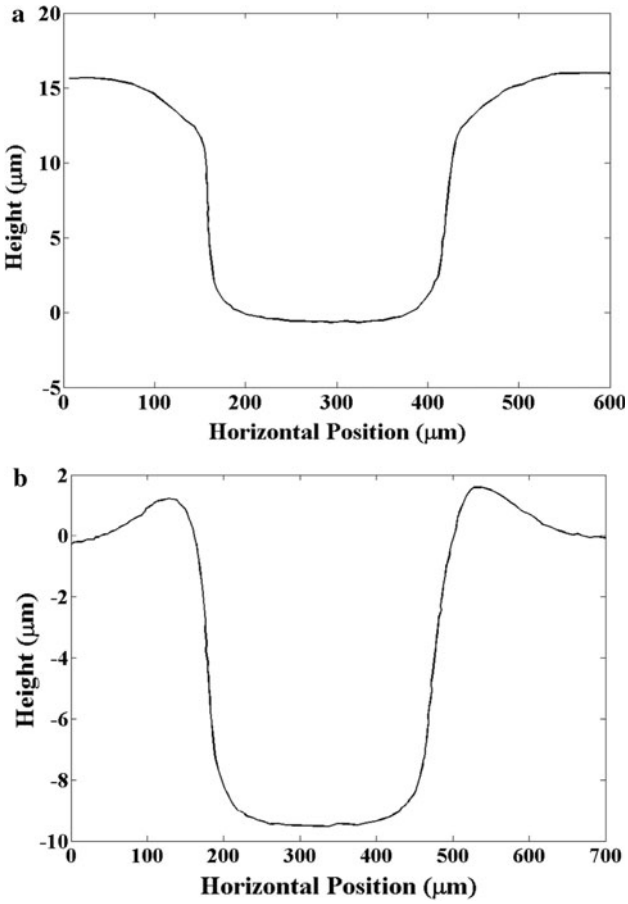

Fig. 8 Surface profilometry depth profile for a section of a micropatterned **a** TPU substrate with MAA sIPN features (20 min soak time) and **b** PDMS substrate with MAA sIPN features (30 min soak time)

such devices were produced from the TPU elastomer substrate (MAA, 10 min soak time) and PDMS elastomer substrate (MAA, 20 min soak time). Channel depth was 16.2 ± 0.2 μm for the TPU and 7.0 ± 0.2 μm for the PDMS. To increase wettability of the surface, the device and the glass cover were briefly treated in an ultraviolet-ozone cleaner to introduce hydrophilic functional groups at the surface. A microfluidic system was created immediately after the UV-ozone treatment by placing the treated glass cover on top of the oxidized elastomer. The adhesive forces between the treated polymer and glass surfaces were sufficient to allow the device to be filled with fluid without maintaining any compressive force. Inlet and outlet holes were punched in the elastomer to allow injection of fluid. Figure 9c illustrates a PDMS device after filling with an aqueous solution of a red dye. The assembly of a functioning microfluidic device with additional components is beyond the scope of this study, but preliminary results illustrate that devices patterned via SIM can be readily converted to microfluidic systems.

3.5 Chemical micropatterning

Besides creating surface wells or channels, SIM processing is also capable of creating chemical patterning in the processed substrate due to the different chemical composition of the IPN and intervening regions. The patterning of carboxylic acid groups within a PDMS-poly(MAA) device is demonstrated here by selective staining of the poly (MAA) with a fluorescent dye. Figure 10a shows fluorescence microscope image of a PDMS elastomer that was infused with a 40 μm checkerboard pattern of poly(MAA). The sample was stained with 6-aminofluorescein, a dye that binds selectively to the –COOH groups of poly(MAA), but does not stain the PDMS (Wang et al. 2005). The bright squares in Fig. 10a correspond to the raised poly(MAA) IPN regions, while the intervening dark regions are PDMS wells. Figure 10b shows a control sample of the same material that was not stained with 6-aminofluorescein. The staining experiments illustrate that surface-accessible functional groups are present in the IPN regions. Micropatterned surface functional groups, including –COOH groups, were previously used to anchor cell-adhesive ligands in several studies of patterned cell growth. Several notable cell biology and tissue engineering studies utilized surface-immobilized proteins or cell-adhesive ligands on micropatterned substrates to control cell adhesion, shape, function, and growth (Tourovskaia et al. 2003; Chen et al. 1998; Folch and Toner 2000; Dike et al. 1999; Folch and Toner 1998; Chin et al. 2004; Revzin et al. 2005; Gopalan et al. 2003; Wang et al. 2005; Cesa et al. 2007; Ghibaudo et al. 2011). SIM may be well-suited for producing flexible, conformable polymeric substrates for cell biology or tissue engineering research due to its ability to create surface chemical patterns on the relevant length scale of 10–100 μm.

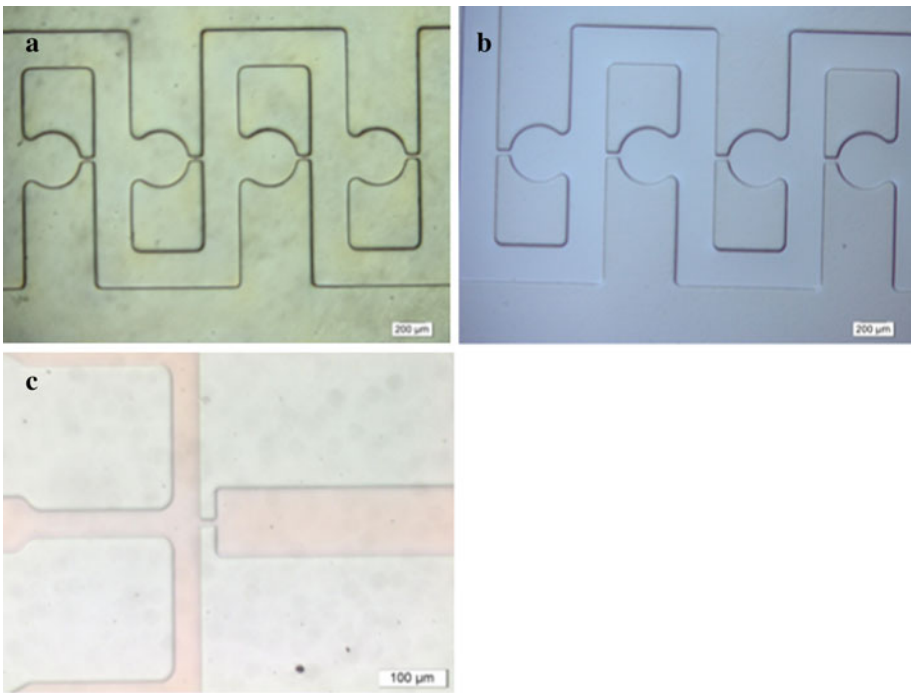

Fig. 9 A finished microfluidic channel system as viewed in an optical microscope (*top view*). **a** TPU substrate with MAA sIPN features (20 min soak time, 16.2 µm depth). **b** PDMS substrate with MAA sIPN features (10 min soak time, 7.0 µm depth). **c** PDMS device with MAA sIPN features, glass cover, after filling with an aqueous solution of a red dye

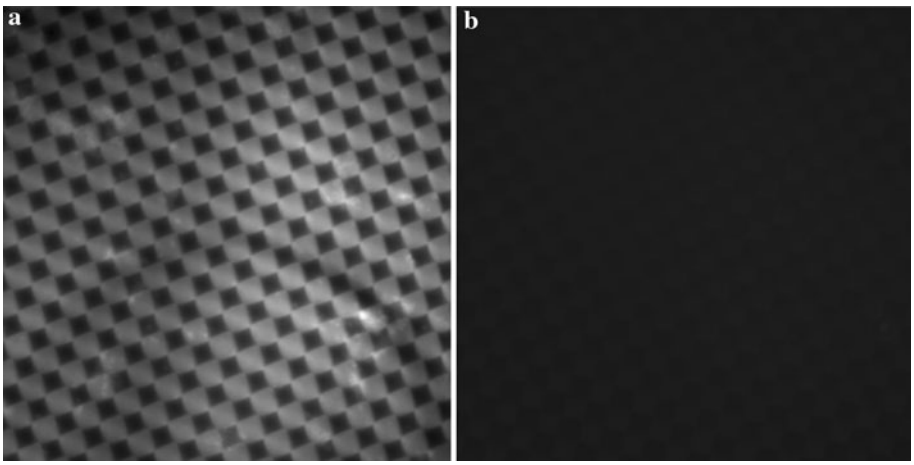

Fig. 10 Demonstration of chemical micropatterning from SIM by selective staining of sIPN regions. **a** Fluorescence image of a PDMS elastomer with 40 µm checkerboard poly(MAA) sIPN pattern. Poly(MAA) sIPN regions were stained with 6-aminofluorescein. **b** Control sample of same without fluorescein staining

3.6 Warpage

A processing issue in SIM is stress imbalance in the final device, which can cause warping or bending of the substrate. If the topmost surface of the elastomer is converted to an IPN or sIPN by UV exposure, while the bottom surface remains underexposed or unexposed, then evaporation of monomer from the bottom surface will cause shrinkage and encourage bending of the substrate during drying. Warpage is undesirable in both microcontact printing and microfluidic applications. Warpage is more noticeable when the substrate is very thin, or when the amount of monomer infused is high. Warpage can be minimized by one of two strategies. One viable approach is choice of a thicker substrate (e.g., 3.2 mm thick TPU instead of 0.32 mm). If monomer infusion depth << substrate thickness, the mechanical rigidity of the substrate material is often enough to overcome residual stresses, so warpage is minimized. Another approach is mounting the elastomer on a rigid glass plate and infusing only the exposed surface with monomer, as described in the Experimental section. For thermoplastic elastomers like the TPU material studied here, it was possible to mount the material on a glass slide by temporarily melting it. Strong adhesion between the TPU and glass prevented delamination of the material during monomer infusion and the processing steps following. The resulting devices were constrained by the glass backing, such that warpage was minimized after SIM processing.

4 Conclusions

SIM is a pseudo-lithographic processing technique that could prove useful for fabrication of microfluidic devices, micropatterned arrays, and microcontact printing devices in a variety of elastomeric substrates, offering the possibility of tuning mechanical properties, optical properties, biological fouling resistance, cell-adhesive properties, and surface wettability. In this report, the patterning of two chemically dissimilar elastomer materials was demonstrated, with promising results. This study focused on readily available, easily polymerizable methacrylate monomers, but other monomers (e.g., vinylic, styrenic, and acrylic monomers) may also prove useful for SIM. Because SIM is applicable to any transparent elastomer that can be swelled with a polymerizable monomer, the range of materials and chemistries accessible is a clear advantage of the technique. SIM is also remarkable for its ability to simultaneously produce topographical and chemical patterning within the surface of the substrate. Importantly, surface chemical patterning cannot be achieved in industrially preferred micropatterning techniques such as hot embossing, injection molding, microthermoforming, and casting without adding an additional surface modification step. Surface chemical patterning is the first step toward designing conformable materials with surface chemical patterning for cell biology or tissue engineering studies, an increasingly important subject in the micropatterning area.

SIM may also prove valuable for its potential to enable rapid scale-up of micropatterned devices from the academic prototype stage to industrial-scale manufacturing. SIM opens the door to fabrication of micropatterned devices from diverse materials with minimal changes to process equipment and methods. Academic research labs have recently shown a strong preference for commercial PDMS elastomers, which are processed by casting, due to the minimal capital equipment cost. However, cast, cross-linked PDMS is not the most readily processable material (or the least expensive) for high-throughput manufacturing. SIM can also be conducted on a low-cost basis at a lab scale with minimal outlay for capital equipment. Because SIM is amenable to processing of materials used for both research lab-level fabrication and mass production, it has the potential to bridge the gap between preferred academic and industrial manufacturing techniques.

The cycle time of the SIM process is a key consideration for manufacturing. Soaking of the elastomer at room temperature for up to 30 min is straightforward and fast enough to be feasible in an academic lab, but for high-throughput manufacturing, the soak time is preferably shorter. For producing shallow channels (1–10 μm depth) in the polymer surface, a monomer soak time of less than 2 min at 40–60°C is possible for many monomers, even though monomer infusion was performed at room temperature for convenience in this study. For deeper channels, longer soak times and higher monomer uptakes are necessary, so cycle time cannot be as short. Besides cycle time, other considerations must be examined in the future to assess the manufacturability of SIM devices, such as strategies for minimizing processing defects and for rapid monomer evaporation and recovery.

Acknowledgments We gratefully acknowledge Bayer MaterialScience LLC for financial support and for providing samples of the TPU material. The authors would like thank Charlie Linch of the TTU Health Sciences Center for the SEM imaging, Dr. Nenad Stojanovic of the TTU Nano Tech Center for optical profilometer measurements, Dr. Vladimir Kuryatkov of the TTU Nano Tech Center for mechanical profilometer measurements, and Swastika Bithi and Deepak Solomon of TTU Chemical Engineering for assisting with Figs. 9c and 10.

References

Abgrall P, Lattes C, Conederal V, Dollat X, Colin S, Gue AM (2006) A novel fabrication method of flexible and monolithic 3D microfluidic structures using lamination of SU-8 films. J Micromech Microeng 16(1):113–121

Agirregabiria M, Blanco FJ, Berganzo J, Arroyo MT, Fullaondo A, Mayora K, Ruano-Lopez JM (2005) Fabrication of SU-8 multilayer microstructures based on successive CMOS compatible adhesive bonding and releasing steps. Lab Chip 5(5):545–552

Ahn CH, Choi JW, Beaucage G, Nevin JH, Lee JB, Puntambekar A, Lee JY (2004) Disposable smart lab on a chip for point-of-care clinical diagnostics. Proc IEEE 92(1):154–173

Alderman BEJ, Mann CM, Steenson DP, Chamberlain JM (2001) Microfabrication of channels using an embedded mask in negative resist. J Micromech Microeng 11(6):703–705

Andersson H, van den Berg A (2003) Microfluidic devices for cellomics: a review. Sens Actuat B Chem 92(3):315–325

Armani DK, Liu C (2000) Microfabrication technology for polycaprolactone, a biodegradable polymer. J Micromech Microeng 10(1):80–84

Barker SLR, Ross D, Tarlov MJ, Gaitan M, Locascio LE (2000) Control of flow direction in microfluidic devices with polyelectrolyte multilayers. Anal Chem 72(24):5925–5929

Becker H, Gartner C (2008) Polymer microfabrication technologies for microfluidic systems. Anal Bioanal Chem 390(1):89–111

Becker H, Heim U (2000) Hot embossing as a method for the fabrication of polymer high aspect ratio structures. Sensor Actuat A Phys 83(1–3):130–135

Becker H, Locascio LE (2002) Polymer microfluidic devices. Talanta 56(2):267–287

Burns MA, Johnson BN, Brahmasandra SN, Handique K, Webster JR, Krishnan M, Sammarco TS, Man PM, Jones D, Heldsinger D, Mastrangelo CH, Burke DT (1998) An integrated nanoliter DNA analysis device. Science 282(5388):484–487

Cesa CM, Kirchgessner N, Mayer D, Schwarz US, Hoffmann B, Merkel R (2007) Micropatterned silicone elastomer substrates for high resolution analysis of cellular force patterns. Rev Sci Instrum 78(3):034301-1–034301-10

Chen CS, Mrksich M, Huang S, Whitesides GM, Ingber DE (1998) Micropatterned surfaces for control of cell shape, position, and function. Biotechnol Prog 14(3):356–363

Chin VI, Taupin P, Sanga S, Scheel J, Gage FH, Bhatia SN (2004) Microfabricated platform for studying stem cell fates. Biotechnol Bioeng 88(3):399–415

Crank J (1968) Diffusion in polymers. Academic Press, New York

Dendukuri D, Doyle PS (2009) The synthesis and assembly of polymeric microparticles using microfluidics. Adv Mater 21(41):4071–4086

Dike LE, Chen CS, Mrksich M, Tien J, Whitesides GM, Ingber DE (1999) Geometric control of switching between growth, apoptosis, and differentiation during angiogenesis using micropatterned substrates. In Vitro Cell Dev Biol Anim 35(8):441–448

El-Ali J, Sorger PK, Jensen KF (2006) Cells on chips. Nature 442(7101):403–411

Folch A, Toner M (1998) Cellular micropatterns on biocompatible materials. Biotechnol Prog 14(3):388–392

Folch A, Toner M (2000) Microengineering of cellular interactions. Annu Rev Biomed Eng 2:227–256

Gadre AP, Nijdam AJ, Garra JA, Monica AH, Cheng MC, Luo C, Srivastava YN, Schneider TW, Long TJ, White RC, Paranjape M, Currie JF (2004) Fabrication of a fluid encapsulated dermal patch using multilayered SU-8. Sensor Actuat A Phys 114(2–3):478–485

Galloway M, Stryjewski W, Henry A, Ford SM, Llopis S, McCarley RL, Soper SA (2002) Contact conductivity detection in poly(methyl methacrylate)-based microfluidic devices for analysis of mono- and polyanionic molecules. Anal Chem 74(10):2407–2415

Gates BD, Xu QB, Stewart M, Ryan D, Willson CG, Whitesides GM (2005) New approaches to nanofabrication: molding, printing, and other techniques. Chem Rev 105:1171–1196

Ghibaudo M, Di Meglio JM, Hersen P, Ladoux B (2011) Mechanics of cell spreading within 3D-micropatterned environments. Lab Chip 11(5):805–812

Giboz J, Copponnex T, Mele P (2007) Microinjection molding of thermoplastic polymers: a review. J Micromech Microeng 17(6):R96–R109

Giselbrecht S, Gietzelt T, Gottwald E, Trautmann C, Truckenmuller R, Weibezahn KF, Welle A (2006) 3D tissue culture substrates produced by microthermoforming of pre-processed polymer films. Biomed Microdevices 8(3):191–199

Gopalan SM, Flaim C, Bhatia SN, Hoshijima M, Knoell R, Chien KR, Omens JH, McCulloch AD (2003) Anisotropic stretch-induced hypertrophy in neonatal ventricular myocytes micropatterned on deformable elastomers. Biotechnol Bioeng 81(5):578–587

Han AR, Wang O, Graff M, Mohanty SK, Edwards TL, Han KH, Frazier AB (2003) Multi-layer plastic/glass microfluidic systems containing electrical and mechanical functionality. Lab Chip 3(3):150–157

Haraldsson KT, Hutchison JB, Sebra RP, Good BT, Anseth KS, Bowman CN (2006) 3D polymeric microfluidic device fabrication via contact liquid photolithographic polymerization (CLiPP). Sensor Actuat B Chem 113(1):454–460

Harrison C, Cabral JT, Stafford CM, Karim A, Amis EJ (2004) A rapid prototyping technique for the fabrication of solvent-resistant structures. J Micromech Microeng 14(1):153–158

Heckele M, Bacher W, Muller KD (1998) Hot embossing—The molding technique for plastic microstructures. Microsyst Technol 4(3):122–124

Hulme JP, Mohr S, Goddard NJ, Fielden PR (2002) Rapid prototyping for injection moulded integrated microfluidic devices and diffractive element arrays. Lab Chip 2(4):203–206

Hutchison JB, Haraldsson KT, Good BT, Sebra RP, Luo N, Anseth KS, Bowman CN (2004) Robust polymer microfluidic device fabrication via contact liquid photolithographic polymerization (CLiPP). Lab Chip 4(6):658–662

Juang YJ, Lee LJ, Koelling KW (2002a) Hot embossing in microfabrication. Part I: experimental. Polym Eng Sci 42(3):539–550

Juang YJ, Lee LJ, Koelling KW (2002b) Hot embossing in microfabrication. Part II: rheological characterization and process analysis. Polym Eng Sci 42(3):551–566

Kameoka J, Craighead HG, Zhang HW, Henion J (2001) A polymeric microfluidic chip for CE/MS determination of small molecules. Anal Chem 73(9):1935–1941

Kameoka J, Orth R, Ilic B, Czaplewski D, Wachs T, Craighead HG (2002) An electrospray ionization source for integration with microfluidics. Anal Chem 74(22):5897–5901

Kim E, Xia YN, Whitesides GM (1996) Micromolding in capillaries: applications in materials science. J Am Chem Soc 118(24): 5722–5731

Kim E, Xia YN, Zhao XM, Whitesides GM (1997) Solvent-assisted microcontact molding: a convenient method for fabricating three-dimensional structures on surfaces of polymers. Adv Mater 9(8):651–654

Kim DS, Lee SH, Ahn CH, Lee JY, Kwon TH (2006) Disposable integrated microfluidic biochip for blood typing by plastic microinjection moulding. Lab Chip 6(6):794–802

Kim J, Junkin M, Kim DH, Kwon S, Shin YS, Wong PK, Gale BK (2009) Applications, techniques, and microfluidic interfacing for nanoscale biosensing. Microfluid Nanofulidics 7(2):149–167

Kricka LJ, Fortina P, Panaro NJ, Wilding P, onso-Amigo G, Becker H (2002) Fabrication of plastic microchips by hot embossing. Lab Chip 2(1):1–4

Kumar A, Whitesides GM (1993) Features of gold having micrometer to centimeter dimensions can be formed through a combination of stamping with an elastomeric stamp and an alkanethiol ink followed by chemical etching. Appl Phys Lett 63(14):2002–2004

Lentz DM (2010) Nanostructured elastomers: from smectic liquid crystals to noble metal nanocomposites. Chapter 3. Ph.D. Thesis, The Pennsylvania State University

Lin CH, Lee GB, Chang BW, Chang GL (2002) A new fabrication process for ultra-thick microfluidic microstructures utilizing SU-8 photoresist. J Micromech Microeng 12(5):590–597

Liu YJ, Ganser D, Schneider A, Liu R, Grodzinski P, Kroutchinina N (2001) Microfabricated polycarbonate CE devices for DNA analysis. Anal Chem 73(17):4196–4201

Liu G, Tian Y, Zhang X (2003) Fabrication of microchannels in negative resist. Microsyst Technol 9(6–7):461–464

Liu KK, Wu RG, Chuang YJ, Khoo HS, Huang SH, Tseng FG (2010) Microfluidic systems for biosensing. Sensors 10(7):6623–6661

Mair DA, Geiger E, Pisano AP, Frechet JMJ, Svec F (2006) Injection molded microfluidic chips featuring integrated interconnects. Lab Chip 6(10):1346–1354

McCormick RM, Nelson RJ, AlonsoAmigo MG, Benvegnu J, Hooper HH (1997) Microchannel electrophoretic separations of DNA in injection-molded plastic substrates. Anal Chem 69(14):2626–2630

McDonald JC, Duffy DC, Anderson JR, Chiu DT, Wu HK, Schueller OJA, Whitesides GM (2000) Fabrication of microfluidic systems in poly(dimethylsiloxane). Electrophoresis 21(1):27–40

Meng ZJ, Qi SZ, Soper SA, Limbach PA (2001) Interfacing a polymer-based micromachined device to a nanoelectrospray ionization Fourier transform ion cyclotron resonance mass spectrometer. Anal Chem 73(6):1286–1291

Metz S, Jiguet S, Bertsch A, Renaud P (2004) Polyimide and SU-8 microfluidic devices manufactured by heat-depolymerizable sacrificial material technique. Lab Chip 4(2):114–120

Nijdam AJ, Monica AH, Gadre AP, Garra JA, Long TJ, Luo C, Cheng MC, Schneider TW, White RC, Paranjape M, Currie JF (2005) Fluidic encapsulation in SU-8 mu-reservoirs with mu-fluidic through-chip channels. Sensor Actuat A Phys 120(1):172–183

Nikcevic I, Lee SH, Piruska A, Ahn CH, Ridgway TH, Limbach PA, Wehmeyer KR, Heineman WR, Seliskar CJ (2007) Characterization and performance of injection molded poly

(methylmethacrylate) microchips for capillary electrophoresis. J Chromatogr A 1154(1–2):444–453
Noerholm M, Bruus H, Jakobsen MH, Telleman P, Ramsing NB (2004) Polymer microfluidic chip for online monitoring of microarray hybridizations. Lab Chip 4(1):28–37
Qu S, Chen XH, Chen D, Yang PY, Chen G (2006) Poly(methyl methacrylate) CE microchips replicated from poly(dimethylsiloxane) templates for the determination of cations. Electrophoresis 27(24):4910–4918
Revzin A, Sekine K, Sin A, Tompkins RG, Toner M (2005) Development of a microfabricated cytometry platform for characterization and sorting of individual leukocytes. Lab Chip 5(1):30–37
Ribeiro JC, Minas G, Turmezei P, Wolffenbuttel RF, Correia JH (2005) A SU-8 fluidic microsystem for biological fluids analysis. Sensor Actuat A Phys 123–24:77–81
Rowland HD, King WP (2004) Polymer deformation and filling modes during microembossing. J Micromech Microeng 14(12):1625–1632
Sato H, Matsumura H, Keino S, Shoji S (2006) An all SU-8 microfluidic chip with built-in 3D fine microstructures. J Micromech Microeng 16(11):2318–2322
Scheer HC, Schulz H (2001) A contribution to the flow behaviour of thin polymer films during hot embossing lithography. Microelectron Eng 56(3–4):311–332
Schulz H, Wissen M, Scheer HC (2003) Local mass transport and its effect on global pattern replication during hot embossing. Microelectron Eng 67–8:657–663
Shah RK, Shum HC, Rowat AC, Lee D, Agresti JJ, Utada AS, Chu LY, Kim JW, Fernandez-Nieves A, Martinez CJ, Weitz DA (2008) Designer emulsions using microfluidics. Mater Today 11(4):18–27
Sia SK, Whitesides GM (2003) Microfluidic devices fabricated in poly(dimethylsiloxane) for biological studies. Electrophoresis 24(21):3563–3576
Sikanen T, Tuomikoski S, Ketola RA, Kostiainen R, Franssila S, Kotiaho T (2005) Characterization of SU-8 for electrokinetic microfluidic applications. Lab Chip 5(8):888–896
Skurtys O, Aguilera JM (2008) Applications of microfluidic devices in food engineering. Food Biophys 3(1):1–15
Squires TM, Quake SR (2005) Microfluidics: fluid physics at the nanoliter scale. Rev Mod Phys 77(3):977–1026
Stone HA, Stroock AD, Ajdari A (2004) Engineering flows in small devices: Microfluidics toward a lab-on-a-chip. Annu Rev Fluid Mech 36:381–411
Svedberg M, Pettersson A, Nilsson S, Bergquist J, Nyholm L, Nikolajeff F, Markides K (2003) Sheathless electrospray from polymer microchips. Anal Chem 75(15):3934–3940
Tay FEH, van Kan JA, Watt F, Choong WO (2001) A novel micromachining method for the fabrication of thick-film SU-8 embedded micro-channels. J Micromech Microeng 11(1):27–32
Toner M, Irimia D (2005) Blood-on-a-chip. Annu Rev Biomed Eng 7:77–103
Tourovskaia A, Barber T, Wickes BT, Hirdes D, Grin B, Castner DG, Healy KE, Folch A (2003) Micropatterns of chemisorbed cell adhesion-repellent films using oxygen plasma etching and elastomeric masks. Langmuir 19(11):4754–4764
Tuomikoski S, Sikanen T, Ketola RA, Kostiainen R, Kotiaho T, Franssila S (2005) Fabrication of enclosed SU-8 tips for electrospray ionization-mass spectrometry. Electrophoresis 26(24):4691–4702
Vanapalli SA, Duits MHG, Mugele F (2009) Microfluidics as a functional tool for cell mechanics. Biomicrofluidics 3(1):012006
Wang YL, Lai HH, Bachman M, Sims CE, Li GP, Allbritton NL (2005) Covalent micropatterning of poly(dimethylsiloxane) by photografting through a mask. Anal Chem 77(23):7539–7546
Whitesides GM (2006) The origins and the future of microfluidics. Nature 442(7101):368–373
Whitesides GM, Ostuni E, Takayama S, Jiang XY, Ingber DE (2001) Soft lithography in biology and biochemistry. Annu Rev Biomed Eng 3:335–373
Xia YN, Whitesides GM (1998) Soft lithography. Angew Chem Int Ed 37(5):551–575
Xu GJ, Yu LY, Lee LJ, Koelling KW (2005) Experimental and numerical studies of injection molding with microfeatures. Polym Eng Sci 45(6):866–875
Yager P, Edwards T, Fu E, Helton K, Nelson K, Tam MR, Weigl BH (2006) Microfluidic diagnostic technologies for global public health. Nature 442(7101):412–418
Young WB (2005) Analysis of the nanoimprint lithography with a viscous model. Microelectron Eng 77(3–4):405–411
Yu LY, Koh CG, Lee LJ, Koelling KW, Madou MJ (2002) Experimental investigation and numerical simulation of injection molding with micro-features. Polym Eng Sci 42(5):871–888
Yu H, Balogun O, Li B, Murray TW, Zhang X (2006) Fabrication of three-dimensional microstructures based on singled-layered SU-8 for lab-on-chip applications. Sensor Actuat A Phys 127(2):228–234